

## Article

# Conditions for and Characteristics of the Dispersion of Gel Fuel Droplets during Ignition

Dmitriy Feoktistov <sup>1</sup>, Evgeniya Orlova <sup>2</sup>, Dmitriy Glushkov <sup>1,\*</sup>, Akram Abedtazehabadi <sup>2</sup>  
and Saveliy Belyaev <sup>1</sup>

<sup>1</sup> Heat and Mass Transfer Laboratory, National Research Tomsk Polytechnic University, 634050 Tomsk, Russia

<sup>2</sup> School of Energy & Power Engineering, National Research Tomsk Polytechnic University, 634050 Tomsk, Russia

\* Correspondence: dmitriyog@tpu.ru

**Abstract:** We formulated and experimentally proved a hypothesis on the causes of dispersion (puffing and microexplosion) of binary fuel droplets, including those in the composition of gel fuels. This hypothesis is based on the concepts of wetting thermodynamics and the theory of the two-component surface energy of substances and materials. An effective and reliable criterion was established that allowed the assessment of the possibility of the onset of puffing and microexplosion during the high-temperature heating of binary liquids. Microexplosions were found to occur only when isothermal conditions were necessarily reached at the liquid–liquid interface during the mixing of mutually insoluble components, provided that one component had to be polar, and the second had to be dispersive. In addition, it was necessary to provide external heating conditions under which the value of the surface free energy of the liquid–liquid interface formation tended to zero.

**Keywords:** gel fuel; emulsion; droplet dispersion; wetting thermodynamics; surface tension; surface free energy



**Citation:** Feoktistov, D.; Orlova, E.; Glushkov, D.; Abedtazehabadi, A.; Belyaev, S. Conditions for and Characteristics of the Dispersion of Gel Fuel Droplets during Ignition. *Appl. Sci.* **2023**, *13*, 1072. <https://doi.org/10.3390/app13021072>

Academic Editor: Adrian Irimescu

Received: 10 December 2022

Revised: 5 January 2023

Accepted: 10 January 2023

Published: 13 January 2023



**Copyright:** © 2023 by the authors. Licensee MDPI, Basel, Switzerland. This article is an open access article distributed under the terms and conditions of the Creative Commons Attribution (CC BY) license (<https://creativecommons.org/licenses/by/4.0/>).

## 1. Introduction

The problem of the negative impact of fossil fuel combustion products on the environment can be solved by using new multicomponent fuel mixtures in practice. They can be prepared in the form of gel fuels [1], emulsions [2], or suspensions [3] containing low-grade solid fuels, waste from coal preparation or oil refining, and water. Compared to fossil fuels, multicomponent fuel mixtures are more environmentally friendly due to the content of water in the fuel mixtures and the effect of its vapor on the chemical reactions that occur during gas-phase combustion [4,5].

Fuel droplets that are widely used in practice (gasoline, kerosene, alcohol, waste oil) are ignited and burned out with a fairly well-studied process of phase transition in the modes of evaporation and boiling of a combustible liquid. Ignition and combustion of multicomponent fuels are accompanied by droplet dispersion (secondary atomization of a droplet) under certain conditions. This is known as puffing and microexplosion [6–8]. Their essence is in the secondary atomization of liquid fuels, which contributes to an increase in the evaporation area of the fuel components and the size of the burnout area, which significantly intensifies ignition and combustion and increases the completeness of fuel burnout. Puffing is characterized by the partial disintegration of a droplet into relatively large fragments. Tsue et al. [6] and Watanbe et al. [7] specifically defined puffing as the process of vapor jet discharge from a fuel droplet's surface. A microexplosion of a two-component droplet—for example, water and a combustible liquid—is characterized by explosive fragmentation of the droplet with the formation of an aerosol [8], which is also known as secondary atomization [9]. Stable microexplosive boiling or puffing occurs when a low-boiling component (usually water) is inside of a high-boiling component (for example,

oil) [10]. That is, a water droplet is covered with a shell of oil. The mechanism of droplet disintegration (puffing and microexplosion) is explained by an increase in temperature at the interface between the low-boiling and high-boiling components, up to the boiling point of the low-boiling component—for example, 100–120 °C for water [11,12]. This strongly depends on the difference in boiling temperatures between oil and water [13]. It is known that if the size of two-component droplets is small, then their evaporation may not be powerful enough to destroy the oil phase for the occurrence of microexplosion [13]. In this case, the puffing mode occurs [7,14]. However, in [10,12,15–19], the authors showed that even partial coalescence can lead to microexplosions. In [8], it was found that puffing and microexplosions occurred under conductive heating conditions and high-density heat fluxes for two-component droplets (water and oil), suspensions, emulsions, and solutions. Under convective heating conditions, these processes were achieved only with the addition of a combustible component (oil) and solid components [8]. Under radiant heating, the droplets disintegrated with the formation of a finely dispersed aerosol and fog (microexplosion), or the droplets monotonously evaporated (at relatively low densities of the supplied radiant heat flux) [8]. The puffing mode was not established in experiments with radiation heating [8]. In [20], air temperature ranges were obtained during convective heating, for which one or another mechanism was implemented—from 300 to 350 °C, puffing occurred, and above 400 °C, microexplosion of the two-component droplets occurred. At the same time, the evaporation surface area of liquid fuels increased by more than 100 times [21]. There were also studies of the puffing and microexplosion of gel fuels based on kerosene [22] and dimethylhydrazine [23].

An analysis of studies [6–20] devoted to the dispersion of fuels showed that its intensity depends on a large number of factors, such as the heat supply mechanism (conductive, convective, radiation), the heating medium's temperature, the concentration of components in the composition of gel fuels, suspensions, emulsions, and solutions, the properties of the components and their ratios in the mixture (solid particles, combustible liquid, water, surfactants), droplet sizes, and the conditions for their formation, which determine the droplet structure (a combustible liquid is the shell, water is the center, or vice versa), as well as the location of the droplet in space (sitting on a surface, on a holder, flying in a gas flow). In real conditions, the dispersion characteristics of multicomponent fuels are affected by a combination of the factors listed above. Therefore, when the conditions of ignition and combustion of such fuels change, individual factors from the above, with their combined effect on the dispersion process, can have a positive effect or weaken this effect. The known results make it possible to establish the dispersion mechanism, which, in general, is reduced to the destruction of vapor bubbles, but they do not allow us to determine the causes, features, and scales of this phenomenon during the ignition and combustion of fuel mixtures. It is also worth noting that the component base of the studied fuels is quite limited and is represented mainly by coals (hard, brown), combustible liquids (kerosene, fuel oil, various types of oils), and one non-combustible liquid (water), which are independent technological energy resources that are widely used on practice. The main concepts of the theory that are applicable in practice for predicting the guaranteed course of droplet dispersion, including fuel mixtures of arbitrary component composition, have not yet been developed.

The purpose of this work was to develop recommendations for the composition of multicomponent droplets (including components that are in composite fuels) for the guaranteed implementation of evaporation, boiling, puffing, or microexplosion under high-temperature heating that is sufficient for the stable ignition of a composite fuel. In this paper, for the first time, the causes of the onset of secondary atomization (puffing and microexplosion) of droplets of multicomponent liquids (including composite fuels) are established based on the concepts of wetting thermodynamics and the theory of the two-component surface energy of substances and materials.

In this work, we will prove a formulated hypothesis that explains the causes of the onset of dispersion (puffing and microexplosion) of droplets under high-temperature heating

that is sufficient for the stable ignition of multicomponent fuels. The hypothesis assumes that the main factor affecting the onset of dispersion (puffing or microexplosion) under high-temperature heating of multicomponent droplets is the mutual solubility/insolubility of the components. The solubility of multicomponent mixtures was estimated based on the well-known approach of “like dissolves like” [24]. This is based on a comparison of the dispersive and polar components of the surface tension of the components that make up the fuels. Surface tension is related to the interaction energy of molecules in the bulk of the condensed phase, the measure of which is the adhesion energy. The work of adhesion is the work that must be done under isothermal conditions to separate the molecules of the condensed phase, i.e., the rupture of the interfacial surface of the components that make up the multicomponent mixture. Weak bonds (van der Waals interactions) are characterized by a dispersive component. The polar component of surface tension characterizes strong bonds between molecules (hydrogen, ionic, covalent, dipole–dipole). Almost all known studies on puffing and microexplosion are carried out on mixtures containing water, which is the most common highly polar substance. As a rule, water is mixed with carbon-containing combustible components, which are non-polar (dispersive) substances. When a polar substance is mixed with a nonpolar one, according to the “like dissolves like” approach, a mixture with mutually insoluble components is formed. When liquid droplets of these mixtures are heated to high temperatures, dispersion (secondary atomization) occurs. That is, puffing or microexplosion occurs only during intense high-temperature heating of a multicomponent droplet when isothermal conditions are reached on the interfacial surface of the components, provided that the polar component predominates in the surface tension of one component (the liquid must be strongly polar:  $\sigma_L^P/\sigma_L^D > 1$ ), and that the dispersive component predominates in the surface tension of the other component (the liquid must be highly dispersive:  $\sigma_L^P/\sigma_L^D \leq 1$ ).

## 2. Materials and Methods

### 2.1. Component Compositions of Liquid Mixtures

To prove the hypothesis formulated in the Introduction, the liquids presented in Table 1 were chosen for experimental studies. Table 1 shows the chemical formulas of the liquids and their manufacturers, boiling points ( $t_b$ ) [25–27], surface tensions ( $\sigma_L$ ), and polar ( $\sigma_L^P$ ) and dispersive ( $\sigma_L^D$ ) parts.

**Table 1.** Characteristics of components in composite fuels.

| Liquid               | Chemical Formula/Boiling Temperature, °C            | Manufacturer   | Reference Data    |                     |                     |      |
|----------------------|---|--|-------------------|---------------------|---------------------|------|
|                      |   |  | $\sigma_L$ , mN/m | $\sigma_L^P$ , mN/m | $\sigma_L^D$ , mN/m | Ref. |
| Water                | H <sub>2</sub> O/100.0                              | Mill-Q water treatment system, Sigma-Aldrich, St. Louis, MO, USA | 72.8              | 51.0                | 21.8                | [28] |
| Monoethanolamine     | C <sub>2</sub> H <sub>7</sub> NO/170.0              | Ekos-1, Moscow, Russia   | 48.2              | 29.4                | 18.8                | [29] |
| Glycerol             | C <sub>3</sub> H <sub>8</sub> O <sub>3</sub> /290.0 | Tula Pharm Factory, Tula, Russia                                 | 63.4              | 26.4                | 37.0                | [28] |
| Ethylene glycol      | C <sub>2</sub> H <sub>6</sub> O <sub>2</sub> /197.3 | Ekos-1, Moscow, Russia   | 47.7              | 16.8                | 30.9                | [28] |
| Acetone              | C <sub>3</sub> H <sub>6</sub> O/56.0                | Ekos-1, Moscow, Russia   | 25.2              | 3.1                 | 22.1                | [30] |
| Ethyl alcohol 95%    | C <sub>2</sub> H <sub>6</sub> O/78.3                | Rosbio, St. Petersburg, Russia                                   | 22.1              | 4.6                 | 17.5                | [31] |
| Diiodomethane        | CH <sub>2</sub> I <sub>2</sub> /182.1               | Alfa Aesar, Heysham, UK  | 50.8              | 0.0                 | 50.8                | [28] |
| Dodecane             | C <sub>12</sub> H <sub>26</sub> /216.3              | Ekos-1, Moscow, Russia   | 25.4              | 0.0                 | 25.4                | [32] |
| Synthetic engine oil | –/190.4   | Gazpromneft, St. Petersburg, Russia                              | 33.4              | 1.4                 | 32.0                | [25] |
| Compressor oil       | –/190.5   | Gazpromneft, St. Petersburg, Russia                              | 28.01             | 0.01                | 28.0                | [25] |
| Oil TEDEX TU 32      | –/208.0   | Gazpromneft, St. Petersburg, Russia                              | 36.1              | 1.1                 | 35.0                | [25] |

### 2.2. Analytical Studies

Insignificant impurities in liquids and environmental conditions significantly affect the surface tension and its parts (polar and dispersive) [33]. Therefore, the surface tension of the liquids was measured, and the parts of the surface tension were calculated. The surface tension of the liquids used in the studies was measured by using a K20 tensiometer (KRUSS, Hamburg, Germany) according to the Du Nouy and Wilhelm methods at a liquid

and ambient temperature of 22 °C. The error in determining the surface tension did not exceed 0.5%, which was several tenths of a mN/m.

According to the Owens, Wendt, Rabel, and Kaelble (work) method, the polar ( $\sigma_L^P$ ) and dispersive ( $\sigma_L^D$ ) parts of the surface tension ( $\sigma_L = \sigma_L^P + \sigma_L^D$ ) of the liquids presented in Table 1 were determined by using the following system of equations [34]:

$$\begin{cases} \frac{\sigma_L(\cos \theta_1 + 1)}{2\sqrt{\sigma_L^D}} = \frac{\sqrt{\sigma_{S1}^P} \cdot \sqrt{\sigma_L^P}}{\sqrt{\sigma_L^D}} + \sqrt{\sigma_{S1}^D} \\ \frac{\sigma_L(\cos \theta_2 + 1)}{2\sqrt{\sigma_L^D}} = \frac{\sqrt{\sigma_{S2}^P} \cdot \sqrt{\sigma_L^P}}{\sqrt{\sigma_L^D}} + \sqrt{\sigma_{S2}^D} \end{cases} \quad (1)$$

where  $\sigma_L$ ,  $\sigma_L^P$ , and  $\sigma_L^D$  are the surface tension and its polar and dispersive parts (target values from Equation (1)) in mN/m;  $\theta_1$  and  $\theta_2$  are static contact angles on test surfaces #1 and #2 (determined experimentally) in  $^\circ$ ;  $\sigma_{S1}^P$ ,  $\sigma_{S1}^D$  and  $\sigma_{S2}^P$ ,  $\sigma_{S2}^D$  are the polar and dispersive parts of the surface free energy (SFE) of test surfaces #1 and #2 (calculated from Equation (2)) in mN/m.

As test surfaces #1 and #2, aluminum–magnesium alloy AMG-6 (ROSTECHKOM, Yekaterinburg, Russia) and fluoropolymer PTFE (APC Group, Yekaterinburg, Russia) were chosen. Surfaces #1 and #2 were made in the form of a disk with a diameter of 50 mm and a thickness of 4 mm, and they had a very low roughness that was close to molecularly smooth. By using the known surface tensions of the test liquids (Table 1), we determined  $\sigma_{S1}^P$ ,  $\sigma_{S1}^D$  and  $\sigma_{S2}^P$ ,  $\sigma_{S2}^D$  by solving the following system:

$$\begin{cases} \frac{\sigma_{L1}(\cos \theta_1 + 1)}{2\sqrt{\sigma_{L1}^D}} = \frac{\sqrt{\sigma_S^P} \cdot \sqrt{\sigma_{L1}^P}}{\sqrt{\sigma_{L1}^D}} + \sqrt{\sigma_S^D} \\ \frac{\sigma_{L2}(\cos \theta_2 + 1)}{2\sqrt{\sigma_{L2}^D}} = \frac{\sqrt{\sigma_S^P} \cdot \sqrt{\sigma_{L2}^P}}{\sqrt{\sigma_{L2}^D}} + \sqrt{\sigma_S^D} \end{cases} \quad (2)$$

where  $\sigma_{L1}$ ,  $\sigma_{L1}^P$ , and  $\sigma_{L1}^D$  are the surface tension of test liquid #1 and its polar and dispersive parts (reference data from Table 1) in mN/m;  $\sigma_{L2}$ ,  $\sigma_{L2}^P$ , and  $\sigma_{L2}^D$  are the surface tension of test liquid #2 and its polar and dispersive parts (reference data from Table 1) in mN/m;  $\theta_1$  and  $\theta_2$  are static contact angles measured on AMG-6/PTFE when wetted by test liquids #1 and #2 (determined experimentally) in  $^\circ$ ;  $\sigma_S^P$  and  $\sigma_S^D$  are the polar and dispersive parts of the SFE of AMG-6/PTFE (target values) in mN/m.

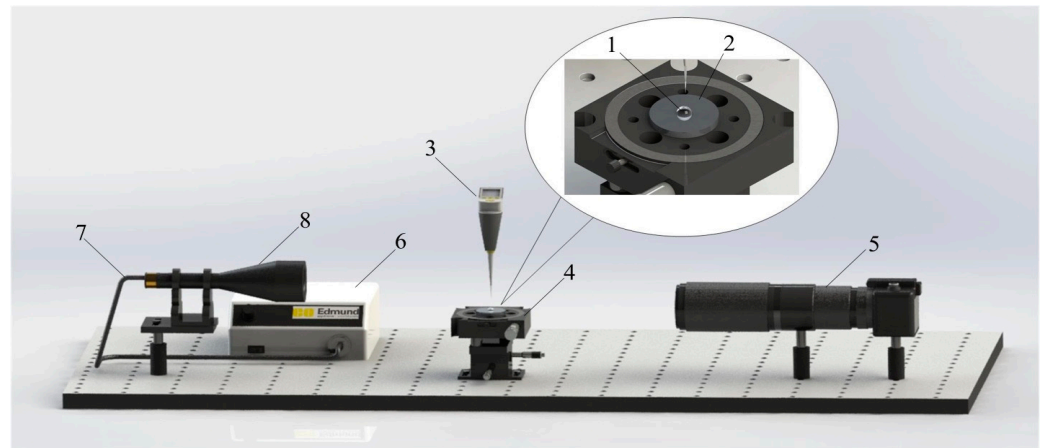
As test liquids, we used liquids with known values of polar and dispersive parts of surface tension (Table 1) [28]. Water was chosen as the test (polar) liquid #1, and diiodomethane was chosen as the test (dispersive) liquid #2.

Table 2 shows the values of the SFE and its polar and dispersive parts for test surfaces #1 (AMG-6) and #2 (PTFE), which were obtained experimentally using the system of Equation (2).

**Table 2.** Surface free energy and its polar and dispersive parts for AMG-6 and PTFE.

| Surface | $\sigma_S$ , mN/m | $\sigma_S^P$ , mN/m | $\sigma_S^D$ , mN/m |
|---------|-------------------|---------------------|---------------------|
| AMG-6   | 29.8              | 3.5                 | 26.3                |
| PTFE    | 19.5              | 0.9                 | 18.6                |

The static contact angles formed by liquid droplets (Table 1) on the surfaces of AMG-6 and PTFE were determined by using a setup in which the shadow optical technique was implemented (Figure 1) [35].



**Figure 1.** Experimental setup for measuring the static contact angles formed by liquid droplets and solid surfaces (AMG-6, PTFE): 1—liquid droplet; 2—AMG-6 or PTFE discs; 3—electronic dispenser; 4—goniometer; 5—camera; 6—light source; 7—fiber optic cable; 8—telecentric tube.

A 5  $\mu\text{L}$  liquid droplet (1) was placed on the surface of AMG-6 or PTFE discs (2) using a Lenpipet Stepper high-precision electronic dispenser (3) (Thermo Scientific, Waltham, MA, USA). An AMG-6 or PTFE disc was placed on a GNL18/M goniometer (4) (ThorLabs, Newton, MA, USA), which made it possible to control the position of the disc in the XY plane. A Nikon D7100 camera (5) (Nikon, Tokyo, Japan) with a Sigma macro lens (105 mm f/2.8 G IF-ED AF-S 9) and a light generation system were used to obtain shadow images of the liquid droplets. The plane-parallel light generation system consisted of an MI-150 light source (6) (Edmund Optics, Barrington, IL, USA), a BX4-type fiber optic cable (7) (Dolan-Jenner, Boxborough, MA, USA), and a 62–760 telecentric tube (8) (Edmund Optics, Barrington, IL, USA). The resulting shadow images of liquid droplets were processed with goniometric methods: LB-ADSA [36] and tangential 1 [37]. The error in determining the contact angles did not exceed 5%.

### 2.3. Experimental Setup for Creating the Conditions for High-Temperature Heating of Liquid Mixtures

Based on an analysis of well-known works [6–20] devoted to the study of dispersion (secondary atomization) of multicomponent droplets, the following main conditions for high-temperature heating of droplets were chosen:

- (1) The heat supply mechanism was mixed (conductive, convective, and radiation);
- (2) The temperature of the heating medium was 900  $^{\circ}\text{C}$ ;
- (3) The number of components in the composition of the droplet and their concentration were two components with a concentration of 50%  $\times$  50% (vol.);
- (4) The droplet formation conditions were intensive mixing of the components at a temperature corresponding to laboratory conditions (from 20 to 24  $^{\circ}\text{C}$ ) for at least 20 min with a magnetic armature rotation speed of at least 1200 rpm;
- (5) The droplet location was on a holder.

The above conditions for conducting the experimental studies of the dispersion of mixture droplets were implemented by using the experimental setup presented in Figure 2.

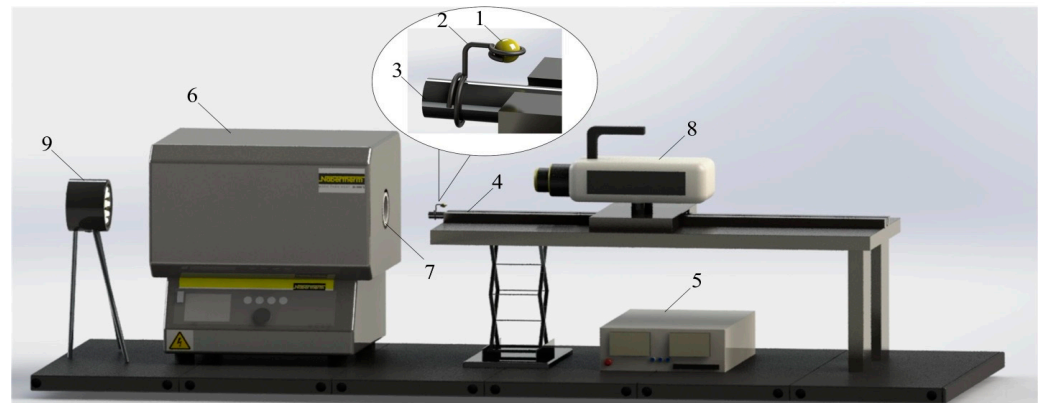


**Figure 2.** Experimental setup: 1—liquid droplet; 2—holder; 3—steel tube; 4—coordinate mechanism; 5—control unit of the coordinate mechanism; 6—muffle furnace; 7—ceramic tube; 8—high-speed video camera; 9—LED lamp.

Binary liquid mixtures were obtained by mixing two of the components listed in Table 1 in a ratio of 50% to 50% (by volume) by using an AIBOTE ZNCLBS-2500 magnetic stirrer (Aibote Henan Science and Technology Development Company, Zhengzhou, China) under laboratory conditions. Stirring was conducted for 20 min at a magnetic armature rotation speed of 1200 rpm. A 10  $\mu\text{L}$  droplet of a binary mixture (1) then was formed on a holder (2) by using a Lenpipet Stepper high-precision electronic dispenser (Thermo Scientific, Waltham, MA, USA). The holder was made of heat-resistant, high-temperature steel wire with a diameter of 500  $\mu\text{m}$ . The holder is fixed on a tube (3) made of steel. A high-precision coordinate mechanism (4) (ZAO Mechatronic Products Plant, Solnechnogorsk, Russia) controlled by an electronic unit (5) was used to move the tube with a holder and a droplet to the center of a tubular muffle furnace (6) (Nabertherm GmbH, Lilienthal, Germany). A temperature of 900  $^{\circ}\text{C}$  inside the ceramic tube (7) was kept constant during the experiments, and it was set and controlled by the built-in controller of the furnace. The high-temperature heating of the droplet was recorded according to a well-tested method [38] by using a V411 high-speed video camera (Vision Research, Wayne, NJ, USA) placed on the coordinate mechanism. A 5-inch LED lamp (9) (Edmund Optics, Barrington, IL, USA) was used to provide the required level of illumination and create a contrast image of the process under study. The video recording was conducted at a speed of at least 2000 fps at a resolution of 800  $\times$  600 pixels. The resulting video files were processed using the Tema Automotive (Image Systems AB, Linkoping, Sweden) and Phantom Camera Control (Vision Research, Wayne, NJ, USA) software according to a well-tested technique [38]. The criterion for the onset of one of the four possible mechanisms (evaporation, boiling, puffing, or microexplosion) during the high-temperature heating of the binary liquid droplets was its steady repetition in at least 70% of the experiments in a series performed under identical conditions. Each series of experiments consisted of 10 repetitions under identical and well-reproducible conditions.

### 3. Results and Discussion

Table 3 shows the experimentally determined values of the surface tension according to the Du Nouy and Wilhelmy methods at a liquid and ambient temperature of 22  $^{\circ}\text{C}$ , as well as the polar and dispersive parts of the surface tension determined according to the OWRK method and their sum. The values of the static contact angles determined when wetting the AMG-6 and PTFE surfaces with the liquids used in the study (Table 3) are presented in the Supplementary Materials.

**Table 3.** Surface tensions of liquids determined by using the Du Nouy and Wilhelmy methods and the polar and dispersive parts of the surface tension and their sum determined by using the OWRK method.

| Liquid   | OWRK Method                    |   | $\sigma_L$ , mN/m (Du Nouy/Wilhelmy Methods) |
|--|--------------------------------|---|--|
|  | $\sigma_L^P/\sigma_L^D$ , mN/m | $\sigma_L = \sigma_L^P + \sigma_L^D$ , mN/m |  |
| <b>First Group (Polar Liquids)</b>   |                                |   |  |
| Water *  | 51.0/21.8                      | 72.80                                       | 72.56 ± 0.03/72.78 ± 0.01                    |
| Monoethanolamine   | 28.8/18.0                      | 46.80                                       | 45.77 ± 0.02/46.00 ± 0.01                    |
| <b>Second Group (Dispersive Liquids with a High Value of the Polar Part)</b> |                                |   |  |
| Glycerol   | 26.0/35.0                      | 61.00                                       | 59.92 ± 0.06/60.88 ± 0.15                    |
| Ethylene glycol  | 17.6/26.4                      | 44.00                                       | 43.52 ± 0.02/43.49 ± 0.01                    |
| <b>Third group (Dispersive Liquids with a Low Value of the Polar Part)</b>   |                                |   |  |
| Acetone  | 2.4/24.1                       | 26.50                                       | 26.12 ± 0.09/25.88 ± 0.02                    |
| Ethyl alcohol 95%  | 3.4/19.0                       | 22.40                                       | 22.08 ± 0.04/22.40 ± 0.01                    |
| <b>Fourth Group (Dispersive Liquids)</b>                                     |                                |   |  |
| Diiodomethane *  | 0.0/50.8                       | 50.80                                       | 49.71 ± 0.02/49.79 ± 0.01                    |
| Dodecane   | 0.01/26.8                      | 26.81                                       | 25.78 ± 0.03/26.10 ± 0.02                    |
| Synthetic engine oil   | 1.2/30.2                       | 31.40                                       | 30.78 ± 0.05/31.50 ± 0.06                    |
| Compressor oil   | 0.01/29.5                      | 29.51                                       | 28.12 ± 0.19/29.7 ± 0.09                     |
| Oil TEDEX TU 32  | 0.8/32.1                       | 32.90                                       | 32.85 ± 0.09/32.84 ± 0.05                    |

\* Test liquids; their values of  $\sigma_L^P$  and  $\sigma_L^D$  were chosen from Ref. [28].

It can be seen from Table 3 that the discrepancy between the surface tension values determined with the Du Nouy, Wilhelmy, and OWRK methods did not exceed 3%. In addition, a comparison of the experimentally established surface tensions and their parts (Table 3) with the known data (Table 1) showed their fairly good reproducibility, as the deviations did not exceed 3%. The deviation from the known data was due to minor impurities and the environmental conditions (mainly the ambient temperature). This indicates the possibility of using the OWRK method to determine the polar and dispersive parts of the surface tension of the liquids used in the study.

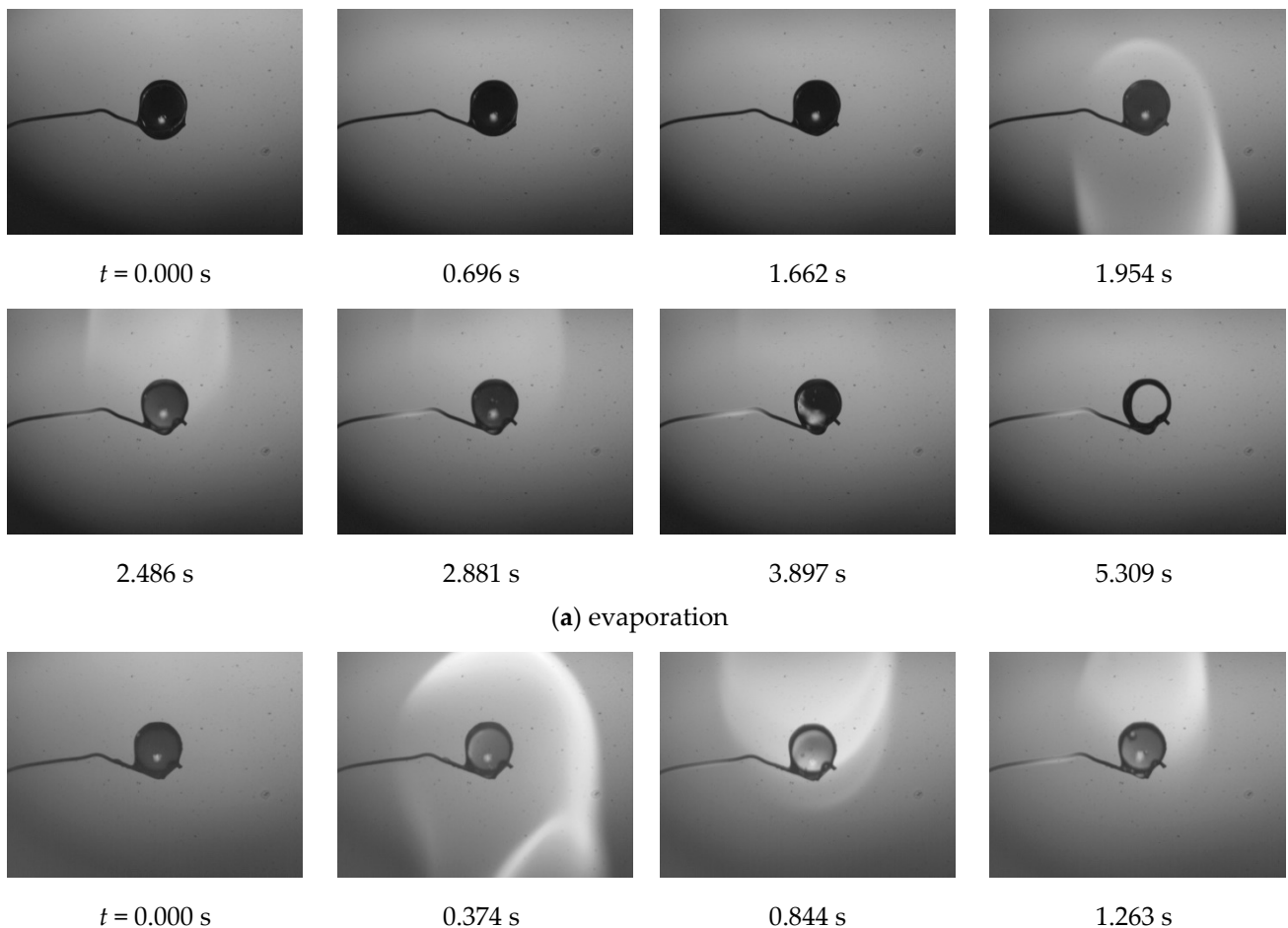
The liquids were conditionally divided into four groups according to the values of the ratio of  $\sigma_L^P/\sigma_L^D$  (Table 3). Water and monoethanolamine, with the predominance of  $\sigma_L^P$  over  $\sigma_L^D$  and a ratio of  $\sigma_L^P/\sigma_L^D > 1$ , were included in the first group of liquids. The second group (dispersive liquids with a high value of the polar part) included glycerol and ethylene glycol, with a ratio of  $0.2 \leq \sigma_L^P/\sigma_L^D \leq 1.0$ . Acetone and ethyl alcohol, with a ratio of  $0.1 \leq \sigma_L^P/\sigma_L^D \leq 0.2$ , were included in the third group of dispersive liquids with a low value of the polar part. Finally, diiodomethane, dodecane, synthetic engine oil, compressor oil, and TEDEX TU 32 oil, with a ratio of  $\sigma_L^P/\sigma_L^D \leq 0.1$ , were included in the fourth group. Thus, we used a dimensionless evaluation criterion ( $\sigma_L^P/\sigma_L^D$ ) that characterized the predominance of bonds between molecules, according to which any liquid could be assigned to one of the four conventionally distinguished groups.

Table 4 presents the experimental results of the study on the onset of one of the four possible mechanisms (evaporation, boiling, puffing, and microexplosion) for droplets of binary mixtures consisting of components (Table 3) subjected to high-temperature heating. Figure 3 presents typical frames of videograms of the studied processes.

**Table 4.** Experimental results of the onset of evaporation, boiling, puffing, and microexplosion for binary liquid droplets subjected to high-temperature heating.

| Composition of Binary Mixture                                    |   | Recorded Process<br>(Evaporation/Boiling/<br>Puffing/Microexplosion) |
|--|---|--|
| Belonging to Groups 1–4<br>(Table 3) of the<br>First Component * | Belonging to Groups 1–4<br>(Table 3) of the<br>Second Component * |  |
| 1st group  | 1st group   | Boiling  |
| 2nd group  | 2nd group   | Boiling  |
| 3rd group  | 3rd group   | Evaporation/Boiling **   |
| 4th group  | 4th group   | Boiling  |
| 1st group  | 2nd group   | Boiling/Puffing **   |
| 1st group  | 3rd group   | Boiling  |
| 1st group  | 4th group   | Microexplosion/Puffing **  |
| 2nd group  | 3rd group   | Boiling  |
| 2nd group  | 4th group   | Puffing/Boiling **   |
| 3rd group  | 4th group   | Boiling  |

\* The liquids from Table 3 were taken as the components. \*\* Boiling or puffing was recorded in 2–3 experiments of the 10 experiments conducted under identical conditions. Microexplosions were recorded in the rest of the 7–8 experiments of the 10 experiments.



**Figure 3.** Cont.

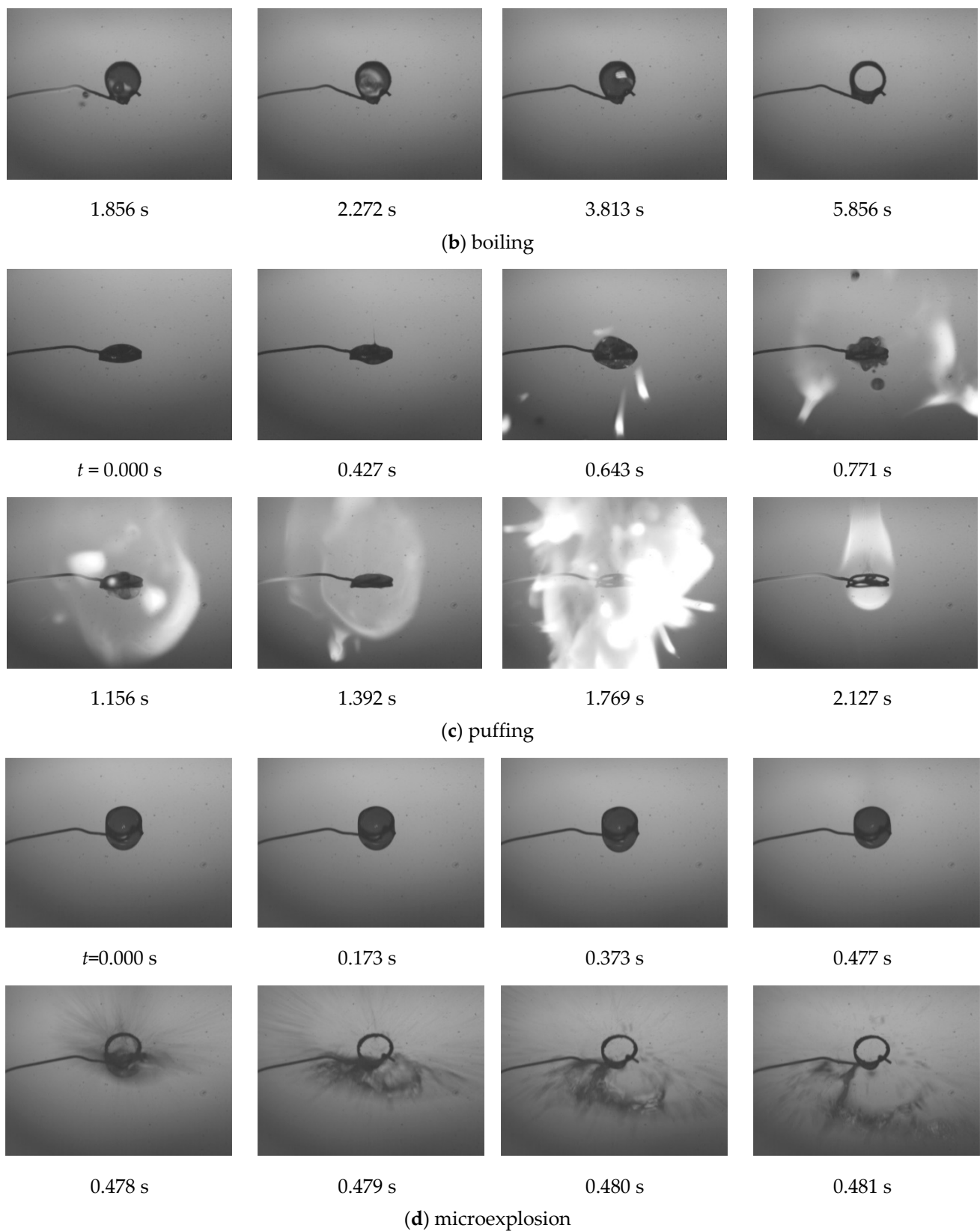


**Figure 3.** Typical frames of videograms illustrating the four mechanisms of physical and chemical processes during the high-temperature heating of binary liquids: (a) evaporation (acetone–95% ethyl alcohol); (b) boiling (water–acetone); (c) puffing (ethylene glycol–compressor oil); (d) microexplosion (monoethylamine–diiodomethane).

According to the “like dissolves like” approach [24], liquids belonging to the same group mutually dissolved. It can be seen from Table 4 that the binary liquid droplets consisting of components characterized by mutual solubility evaporated or boiled. A phase transition in the evaporation mode (without boiling/puffing/microexplosion) was recorded during the heating of a droplet consisting of components from the third group (dispersive liquids with a low value of the polar part). This was due to the fact that liquids belonging to the third group had low boiling points (Table 1) and, consequently, a high evaporation rate. Under the conditions of the experiments, the boiling of binary liquid droplets consisting of components from the third group was suppressed due to intense evaporation and, as a result, a significant removal of heat from the droplets, which was necessary to heat the droplets to the boiling temperature and form nucleation centers. It is also worth noting that the boiling of binary liquids that included components of the same group was realized without the separation of fragments from the parent droplet during the destruction of the vapor bubble. This means that there was no puffing during the destruction of the vapor bubbles formed during boiling. This indicates that the causes of the vapor bubbles’ nucleation, further degradation, and destruction, as well as the characteristics of the vapor bubbles formed during boiling, puffing, and microexplosion, were different. They were connected with the component compositions of the droplets (mutual solubility/insolubility of the components).

Stable (at least 7 out of 10 experiments) puffing was recorded during the high-temperature heating of binary liquid droplets consisting of components from the second and fourth groups. Puffing was also recorded during the heating of droplets consisting of components from the first and second groups, as well as the first and fourth groups, but puffing was not stable for these mixtures. This indicates that puffing could occur under these conditions, and when using these mixtures (first and second groups and first and fourth groups), but for the stable onset, it was necessary to achieve isothermal conditions at the interface of the components.

Droplet microexplosions were recorded only under the conditions of mixing components from the first and fourth groups with all possible combinations of components (water–diiodomethane/dodecane/synthetic machine oil/compressor Oil/TEDEX TU 32 oil or monoethanolamine–diiodomethane/dodecane/synthetic machine oil/compressor oil/TEDEX oil). That is, they were only recorded when mixing two components characterized by high mutual insolubility due to the predominance of the polar part ( $\sigma_L^P/\sigma_L^D > 1$ ) in the surface tension in one component and the dispersive part ( $\sigma_L^P/\sigma_L^D \leq 0.1$ ) in the other component.

It should be noted that during the high-temperature heating of droplets consisting of components from the first and third, second and third, or third and fourth groups in all possible combinations, boiling was realized, despite the fact that the components of these binary mixtures were included in different groups (characterized by partial mutual insolubility). Boiling was explained by the fact that the droplet component composition included a liquid from the third group, which had low boiling point and high evaporation rate compared to those from the first, second, and fourth groups. Under high-temperature heating, the volatile liquids from the third group mainly evaporated. Therefore, vapor bubbles were formed under conditions when the component from the third group almost completely evaporated. This indicates that, in addition to a significant difference in  $\sigma_L^P$  and  $\sigma_L^D$  for the components, one more condition must be met for the onset of puffing or microexplosion. This condition is the achievement of isothermal conditions at the liquid–liquid interface. Under isothermal conditions, the energy supplied to the droplet will ensure the growth of nucleation centers on the intercomponent interface. Their further destruction (collapse) will lead to puffing or microexplosion. According to the formulated hypothesis, it should be noted that the mixing of the components from the third group with components from other groups can lead to puffing, but superhigh heat fluxes can be supplied to a droplet of a binary liquid in a very short period of time, for example, by heating the droplet with laser radiation.

Based on the experimental results, a hypothesis was formulated about the causes of the microexplosive dispersion of binary liquid droplets under their intense heating. This hypothesis is based on the thermodynamics of wetting, as well as the theory of two-component SFE. The SFE of the liquid–liquid interface formation in the general case can be defined as:

$$\Delta G_{1,2} = \sigma_{1,2} - \sigma_{L1} - \sigma_{L2} = -2 \left[ \left( \sigma_{L1}^D \cdot \sigma_{L2}^D \right)^{1/2} + \left( \sigma_{L1}^P \cdot \sigma_{L2}^P \right)^{1/2} \right] \quad (3)$$

where  $\sigma_{1,2}$  is the interfacial tension at the liquid–liquid interface in N/m;  $\sigma_{L1}$  and  $\sigma_{L2}$  are surface tensions of liquids (components) #1 and #2, respectively in N/m.

The surface free energy of the liquid–liquid interface formation had a negative value in the vast majority of the cases of the mixing of two liquids. Table S2 presents the values of the SFE of the liquid–liquid interface formation. The formation of the liquid–liquid interface is less energy-intensive than the formation of the liquid–gas interface from the point of view of thermodynamics. This is due to the fact that liquids have cohesive interactions between their molecules at the liquid–gas interface. There are no cohesive interactions between gas molecules. Molecules on the surface of a liquid tend to interact with any other liquid, but not gas molecules. The last statement was also valid in the case of mutually insoluble liquids when the components from the first group (polar liquids) and fourth group (dispersive liquids) were mixed. Let us consider the mixing of the components of these groups in more detail. Molecules of liquids belonging to the fourth group were only capable of relatively weak van der Waals interactions; in addition, they were capable of much stronger hydrogen bond interactions. Consequently, the molecules of the liquids from the first group would prefer to interact with each other than with the molecules of liquids from the fourth group. However, the molecules of the liquids in the first group at the liquid–gas interface were forced to interact with the gas (the environment, under the conditions of the experiments with air). Under the action of cohesive forces, the molecules of the liquids from the first group tended to lower the surface energy. Under such conditions, the inversion of the “liquid–gas” interaction into a liquid–liquid interaction occurred upon contact with any other liquid. This was true even when the interaction was conducted predominantly by van der Waals forces, as in the case of the liquids from the fourth group. Therefore, the SFE of the liquid–liquid interface formation when mixing components from the first and fourth groups would always be negative. It should be noted that the SFE of the liquid–liquid interface formation took on more negative values if two liquids were mutually soluble (capable of similar cohesive interactions)—for example, components belonging to the same group or components from the first and second groups. That is, the energy tended to the lowest values under conditions in which the liquids were characterized by close values of  $\sigma_L^P$  and  $\sigma_L^D$ .

Under the conditions of high-temperature heating, the heat supplied to the binary liquid droplets was spent on its heating and evaporation. As the droplets heated up, their temperature rose. As the temperature rose, the surface tension of the components that made up the mixture decreased. Consequently, the SFE of the liquid–liquid interface formation decreased. The condition for the formation of a vapor bubble on the liquid–liquid interface was a decrease in the SFE (under ideal conditions) and the implementation of isothermal conditions. This would occur when the heat accumulated in the droplet exceeded the heat spent to heat the droplet to the boiling point of the low-boiling component and compensated for the heat spent on the evaporation of the components that made up the droplet.

Below, we formulate the main concepts for the prognostic assessment of the onset of one of the four possible mechanisms of physical and chemical processes during the high-temperature heating of binary liquid droplets:

- I. Monotonic evaporation occurs if none of the components that make up the binary liquid reach the boiling point.
- II. The boiling of binary liquids occurs if only the low-boiling component that is part of the component composition of the mixture reaches the boiling point during

- heating. This is realized by mixing liquid components within one group with the mutual solubility of the components: polar; dispersive with a high value of the polar part; dispersive with a low value of the polar part; dispersive. This also occurs by mixing liquid components with partial solubility within the different groups identified above—first group + second group; first group + third group; second group + third group; second group + fourth group; third group + fourth group—when isothermal conditions are not reached at the liquid–liquid interface.
- III. Puffing occurs by mixing insoluble (or poorly soluble) liquid components that are characterized by a significant difference between the polar and dispersive parts of surface tension and with the obligatory achievement of isothermal conditions at the liquid–liquid interface. Puffing can occur by mixing components in the following combinations of groups: first group + fourth group; first group + second group; second group + fourth group.
- IV. Microexplosions occur only when isothermal conditions are necessarily reached at the liquid–liquid interface when mutually insoluble components are mixed, and one component must be characterized by the ratio of  $\sigma_L^P/\sigma_L^D > 1$  (must be polar), and the second by the ratio of  $\sigma_L^P/\sigma_L^D \leq 0.1$  (must be dispersive). In addition, it is necessary to provide external heating conditions under which the value of the SFE of the liquid–liquid interface formation tends to zero.

It should be noted that according to the formulated hypothesis about the causes of puffing or microexplosion, such factors as the method of supplying heat to the droplet, the temperature of the heating medium, the concentrations of components and their ratio in the composition of the droplet, the size of the droplets, the conditions for their formation, and the location of the droplet are not the causes of puffing or microexplosion. They are only factors affecting the implementation of isothermal conditions at the liquid–liquid interface and affecting the size of the liquid–liquid interface’s surface area, on which the intensity of puffing or microexplosion depends. The composition of multicomponent fuel mixtures, including gel fuels, can vary quite widely in a wide range of components. Without conducting expensive, time-consuming experimental studies on puffing and microexplosion, it is possible to evaluate the influence of components on the possible onset of puffing or microexplosion with the values of the polar and dispersive components of surface tension.

#### 4. Conclusions

It was experimentally proven that the main factor influencing the onset of dispersion (puffing or microexplosion) under the high-temperature heating of multicomponent droplets is the mutual solubility/insolubility of the components. Puffing occurs by mixing insoluble (or poorly soluble) liquid components that are characterized by a significant difference between the polar and dispersive parts of surface tension and with the obligatory achievement of isothermal conditions at the liquid–liquid interface. Microexplosions occur only when isothermal conditions are necessarily reached at the liquid–liquid interface when mutually insoluble components are mixed, and one component must be characterized by the ratio of  $\sigma_L^P/\sigma_L^D > 1$  (must be polar), and the second by the ratio of  $\sigma_L^P/\sigma_L^D \leq 0.1$  (must be dispersive). In addition, it is necessary to provide external heating conditions under which the value of the SFE of the liquid–liquid interface formation tends to zero.

The results obtained in this work contribute not only to the development of fundamental science in the field of dispersion (secondary atomization) of droplets, but also to the development of promising industrial technologies based on secondary droplet atomization. These technologies include: (1) in industrial heat power engineering, energy-efficient methods of combustion under conditions of microexplosive dispersion of droplets of composite fuels; (2) in metallurgy, a method for removing high heat fluxes from the surfaces of a continuously cast billet under conditions of microexplosive dispersion of droplets of non-combustible emulsions and suspensions when they spray the slab surface in the secondary cooling zone of continuous casting machines; (3) in digital, intelligent production

technologies, a cooling method based on microexplosive dispersion of coolant droplets for microelectronic devices whose surfaces emit high heat fluxes (up to 1000 W/cm<sup>2</sup>).

**Supplementary Materials:** The following supporting information can be downloaded at: <https://www.mdpi.com/article/10.3390/app13021072/s1>, Table S1: Static contact angles ( $\theta \pm \Delta\theta$ ) formed by droplets of studied liquids and surfaces of AMG-6 and PTFE; Table S2: Surface free energy the liquid-liquid interface formation.

**Author Contributions:** Conceptualization, D.F. and D.G.; methodology, E.O.; validation A.A.; investigation, S.B.; data curation, D.F.; writing—original draft preparation, E.O. and D.F.; writing—review and editing, D.G.; visualization, A.A.; supervision, D.G.; funding acquisition, D.G. All authors have read and agreed to the published version of the manuscript.

**Funding:** This research was supported by the Russian Science Foundation (grant number 18-13-00031, <https://rscf.ru/project/21-13-28043/> (accessed on 10 December 2022)).

**Conflicts of Interest:** The authors declare no conflict of interest.

## Abbreviations

|               |   |
|---------------|---|
| SFE           | surface free energy   |
| Greek symbols |   |
| $\sigma$      | surface tension for liquid, surface free energy for solid, mN/m |
| $\theta$      | static contact angle, °   |
| $t_b$         | boiling temperature, °C   |
| Subscripts    |   |
| $L$           | liquid  |
| $S$           | solid (surface)   |
| $P$           | polar part  |
| $D$           | dispersive part   |
| 1,2           | serial number of the test liquid/surface                        |

## References

1. Feoktistov, D.V.; Glushkov, D.O.; Kuznetsov, G.V.; Orlova, E.G. Gel Fuels Based on Oil-Filled Cryogels: Corrosion of Tank Material and Spontaneous Ignition. *Chem. Eng. J.* **2020**, *421*, 127765. [\[CrossRef\]](#)
2. Kadota, T.; Yamasaki, H. Recent Advances in the Combustion of Water Fuel Emulsion. *Prog. Energy Combust. Sci.* **2002**, *28*, 385–404. [\[CrossRef\]](#)
3. Khanpit, V.; Tajane, S.P.; Mandavgane, S.A. Experimental Studies on Coal-Water Slurry Fuel Prepared from Pretreated Low-Grade Coal. *Int. J. Coal Prep. Util.* **2022**, *42*, 831–845. [\[CrossRef\]](#)
4. Glushkov, D.O.; Nyashina, G.S.; Anand, R.; Strizhak, P.A. Composition of Gas Produced from the Direct Combustion and Pyrolysis of Biomass. *Process Saf. Environ. Prot.* **2021**, *156*, 43–56. [\[CrossRef\]](#)
5. Nyashina, G.S.; Vershinina, K.Y.; Shlegel, N.E.; Strizhak, P.A. Effective Incineration of Fuel-Waste Slurries from Several Related Industries. *Environ. Res.* **2019**, *176*, 108559. [\[CrossRef\]](#) [\[PubMed\]](#)
6. Tsue, M.; Segawa, D.; Kadota, T.; Yamasaki, H. Observation of Sooting Behavior in an Emulsion Droplet Flame by Planar Laser Light Scattering in Microgravity. *Symp. Combust.* **1996**, *26*, 1251–1258. [\[CrossRef\]](#)
7. Watanabe, H.; Harada, T.; Matsushita, Y.; Aoki, H.; Miura, T. The Characteristics of Puffing of the Carbonated Emulsified Fuel. *Int. J. Heat Mass Transf.* **2009**, *52*, 3676–3684. [\[CrossRef\]](#)
8. Antonov, D.V.; Kuznetsov, G.V.; Strizhak, P.A. Differences of Two-Component Droplets Breakup at the High Temperatures. *J. Energy Inst.* **2020**, *93*, 351–366. [\[CrossRef\]](#)
9. Pilch, M.; Erdman, C.A. Use of Breakup Time Data and Velocity History Data to Predict the Maximum Size of Stable Fragments for Acceleration-Induced Breakup of a Liquid Drop. *Int. J. Multiph. Flow* **1987**, *13*, 741–757. [\[CrossRef\]](#)
10. Mura, E.; Massoli, P.; Josset, C.; Loubar, K.; Bellettre, J. Study of the Micro-Explosion Temperature of Water in Oil Emulsion Droplets during the Leidenfrost Effect. *Exp. Therm. Fluid Sci.* **2012**, *43*, 63–70. [\[CrossRef\]](#)
11. Strizhak, P.A.; Piskunov, M.V.; Volkov, R.S.; Legros, J.C. Evaporation, Boiling and Explosive Breakup of Oil–Water Emulsion Drops under Intense Radiant Heating. *Chem. Eng. Res. Des.* **2017**, *127*, 72–80. [\[CrossRef\]](#)
12. Volkov, R.S.; Strizhak, P.A. Using Planar Laser Induced Fluorescence to Explore the Mechanism of the Explosive Disintegration of Water Emulsion Droplets Exposed to Intense Heating. *Int. J. Therm. Sci.* **2018**, *127*, 126–141. [\[CrossRef\]](#)
13. Moussa, O.; Tarlet, D.; Massoli, P.; Bellettre, J. Parametric Study of the Micro-Explosion Occurrence of W/O Emulsions. *Int. J. Therm. Sci.* **2018**, *133*, 90–97. [\[CrossRef\]](#)

14. Shinjo, J.; Xia, J.; Ganippa, L.C.; Megaritis, A. Physics of Puffing and Microexplosion of Emulsion Fuel Droplets. *Phys. Fluids* **2014**, *26*, 103302. [[CrossRef](#)]
15. Califano, V.; Calabria, R.; Massoli, P. Experimental Evaluation of the Effect of Emulsion Stability on Micro-Explosion Phenomena for Water-in-Oil Emulsions. *Fuel* **2014**, *117*, 87–94. [[CrossRef](#)]
16. Suzuki, Y.; Harada, T.; Watanabe, H.; Shoji, M.; Matsushita, Y.; Aoki, H.; Miura, T. Visualization of Aggregation Process of Dispersed Water Droplets and the Effect of Aggregation on Secondary Atomization of Emulsified Fuel Droplets. *Proc. Combust. Inst.* **2011**, *33*, 2063–2070. [[CrossRef](#)]
17. Yahaya Khan, M.; Abdul Karim, Z.A.; Aziz, A.R.A.; Heikal, M.R.; Crua, C. Puffing and Microexplosion Behavior of Water in Pure Diesel Emulsion Droplets During Leidenfrost Effect. *Combust. Sci. Technol.* **2017**, *189*, 1186–1197. [[CrossRef](#)]
18. Jarvis, T.J.; Donohue, M.D.; Katz, J.L. Bubble Nucleation Mechanisms of Liquid Droplets Superheated in Other Liquids. *J. Colloid Interface Sci.* **1975**, *50*, 359–368. [[CrossRef](#)]
19. Yahaya Khan, M.; Abdul Karim, Z.A.; Aziz, A.R.A.; Tan, I.M. Experimental Study on Influence of Surfactant Dosage on Micro Explosion Occurrence in Water in Diesel Emulsion. *Appl. Mech. Mater.* **2016**, *819*, 287–291. [[CrossRef](#)]
20. Antonov, D.V.; Piskunov, M.V.; Strizhak, P.A. Breakup and Explosion of Droplets of Two Immiscible Fluids and Emulsions. *Int. J. Therm. Sci.* **2019**, *142*, 30–41. [[CrossRef](#)]
21. Antonov, D.V.; Volkov, R.S.; Strizhak, P.A. An Explosive Disintegration of Heated Fuel Droplets with Adding Water. *Chem. Eng. Res. Des.* **2018**, *140*, 292–307. [[CrossRef](#)]
22. Cao, Q.; Liao, W.; Wu, W.T.; Feng, F. Combustion Characteristics of Inorganic Kerosene Gel Droplet with Fumed Silica as Gellant. *Exp. Therm. Fluid Sci.* **2019**, *103*, 377–384. [[CrossRef](#)]
23. Feng, S.; He, B.; He, H.; Su, L.; Hou, Z.; Nie, W.; Guo, X. Experimental Studies the Burning Process of Gelled Unsymmetrical Dimethylhydrazine Droplets under Oxidant Convective Conditions. *Fuel* **2013**, *111*, 367–373. [[CrossRef](#)]
24. Zhuang, B.; Ramanauskaite, G.; Koa, Z.Y.; Wang, Z.G. Like Dissolves like: A First-Principles Theory for Predicting Liquid Miscibility and Mixture Dielectric Constant. *Sci. Adv.* **2021**, *7*, 7275–7287. [[CrossRef](#)] [[PubMed](#)]
25. Glushkov, D.O.; Feoktistov, D.V.; Kuznetsov, G.V.; Batishcheva, K.A.; Kudelova, T.; Paushkina, K.K. Conditions and Characteristics of Droplets Breakup for Industrial Waste-Derived Fuel Suspensions Ignited in High-Temperature Air. *Fuel* **2020**, *265*, 116915. [[CrossRef](#)]
26. Vargaftik, N.B. *Handbook of Thermophysical Properties of Gases and Liquids*; Alekseev, V.A., Ed.; Nauka: Moscow, Russia, 1972.
27. Volkov, A.I.; Zharsky, I.M. *Big Chemical Reference Book*; Modern School: Minsk, Belarus, 2005; ISBN 985-6751-04-7.
28. Ström, G.; Fredriksson, M.; Stenius, P. Contact Angles, Work of Adhesion, and Interfacial Tensions at a Dissolving Hydrocarbon Surface. *J. Colloid Interface Sci.* **1987**, *119*, 352–361. [[CrossRef](#)]
29. Panzer, J. Components of Solid Surface Free Energy from Wetting Measurements. *J. Colloid Interface Sci.* **1973**, *44*, 142–161. [[CrossRef](#)]
30. Nahum, T.; Dodiuk, H.; Kenig, S.; Panwar, A.; Barry, C.; Mead, J. The Effect of Composition and Thermodynamics on the Surface Morphology of Durable Superhydrophobic Polymer Coatings. *Nanotechnol. Sci. Appl.* **2017**, *10*, 53. [[CrossRef](#)]
31. Koerner, G.; Rossmly, G.; Sanger, G. Oberflächen und Grenzflächen. Ein Versuch, die physikalisch-chemischen Grundgrößen darzustellen und sie mit Aspekten der Anwendungstechnik zu verbinden. In *Goldschmidt Informiert Essen No. 29*; Goldschmidt AG: Essen, Germany, 1974.
32. Jie-Rong, C.; Wakida, T. Studies on the Surface Free Energy and Surface Structure of PTFE Film Treated with Low Temperature Plasma. *J. Appl. Polym. Sci.* **1997**, *63*, 1733–1739. [[CrossRef](#)]
33. Boinovich, L.B.; Emelyanenko, A.M. Experimental Determination of the Surface Energy of Polycrystalline Ice. *Dokl. Phys. Chem.* **2014**, *459*, 198–202. [[CrossRef](#)]
34. Owens, D.K.; Wendt, R.C. Estimation of the Surface Free Energy of Polymers. *J. Appl. Polym. Sci.* **1969**, *13*, 1741–1747. [[CrossRef](#)]
35. Kuznetsov, G.V.; Islamova, A.G.; Orlova, E.G.; Ivashutenko, A.S.; Shanenkov, I.I.; Zykov, I.Y.; Feoktistov, D.V. Influence of Roughness on Polar and Dispersed Components of Surface Free Energy and Wettability Properties of Copper and Steel Surfaces. *Surf. Coat. Technol.* **2021**, *422*, 127518. [[CrossRef](#)]
36. Hoorfar, M.; Neumann, A.W. Recent Progress in Axisymmetric Drop Shape Analysis (ADSA). *Adv. Colloid Interface Sci.* **2006**, *121*, 25–49. [[CrossRef](#)] [[PubMed](#)]
37. Bateni, A.; Susnar, S.S.; Amirfazli, A.; Neumann, A.W. A High-Accuracy Polynomial Fitting Approach to Determine Contact Angles. *Colloids Surf. A Physicochem. Eng. Asp.* **2003**, *219*, 215–231. [[CrossRef](#)]
38. Feoktistov, D.V.; Glushkov, D.O.; Kuznetsov, G.V.; Nikitin, D.S.; Orlova, E.G.; Paushkina, K.K. Ignition and Combustion Characteristics of Coal-Water-Oil Slurry Placed on Modified Metal Surface at Mixed Heat Transfer. *Fuel Process. Technol.* **2022**, *233*, 107291. [[CrossRef](#)]

**Disclaimer/Publisher's Note:** The statements, opinions and data contained in all publications are solely those of the individual author(s) and contributor(s) and not of MDPI and/or the editor(s). MDPI and/or the editor(s) disclaim responsibility for any injury to people or property resulting from any ideas, methods, instructions or products referred to in the content.